

Pop III Supernova Feedback on the Formation of the First Galaxies

Li-Hsin Chen^{1,2} and Ke-Jung Chen¹

¹Institute of Astronomy and Astrophysics, Academia Sinica, P.O. Box 23-141, Taipei 10617, Taiwan

²Institute of Astrophysics, National Taiwan University, Taipei 10617, Taiwan

Abstract. Modern cosmological simulations suggest that the hierarchical assembly of dark matter halos provided the gravitational wells that allowed the primordial gases to form stars and galaxies inside them. The first galaxies comprised of the first systems of stars gravitationally bound in dark matter halos are naturally recognized as the building blocks of early Universe. To understand the formation of the first galaxies, we use an adaptive mesh refinement (AMR) cosmological code, *Enzo* to simulate the formation and evolution of the first galaxies. We first model an isolated galaxy by considering much microphysics such as star formation, stellar feedback, and primordial gas cooling. To examine the effect of Pop III stellar feedback to the first galaxy formation, we adjust the initial temperature, density distribution and metallicity distributions by assuming different IMFs of the first stars. Our results suggest that star formation in the first galaxies is sensitive to the initial conditions of Pop III supernovae and their remnants. Our study can help to correlate the populations of the first stars and supernovae to star formation inside these first galaxies which may be soon observed by the (James Webb Space Telescope JWST).

Keywords. methods: numerical, galaxies: formation, galaxies: evolution, (ISM:) supernova remnant

1. Introduction

Recent theoretical studies suggest that the first galaxies form about several hundred million years after the Big Bang. The next generation of facilities such as *James Webb Space Telescope (JWST)* will be able to probe the Universe at redshift $\gtrsim 10$. If these first galaxies are bright enough, they are likely to be observed by such the coming big telescopes. The key to understand the formation of the first galaxies is to study the chemical and radiative feedback from the stars formed prior to them. In this work, we aim to study the influence of the first supernovae by testing different Pop III initial mass functions (IMFs) on the Pop II star formation inside the first galaxies. We mainly simulate the merging process of the Pop III supernova remnants (SNR) in an isolated galaxy. Therefore, our simulations achieve a much higher resolution than other typical cosmological simulations. The initial conditions are constructed manually to examine the effect of different assumptions of Pop III IMF.

2. Numerical Setup

We perform the simulations using the adaptive mesh refinement code *Enzo*. Our simulation includes a dark matter halo with an NFW profile, self-gravity of baryon, and chemical cooling. The fiducial setup for our halo is with a mass of $10^9 M_{\odot}$ and a 1 kpc

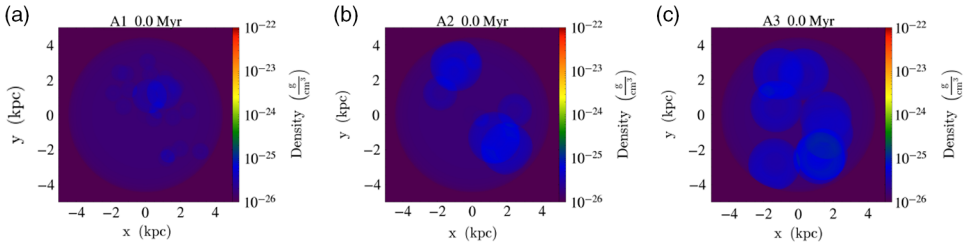


Figure 1. Density-weighted projection plots of the initial gas density distribution of three simulations. Left, middle and right panels show model A1 (Salpeter IMF), model A2 (Flat IMF), model A3 (Hirano IMF), respectively.

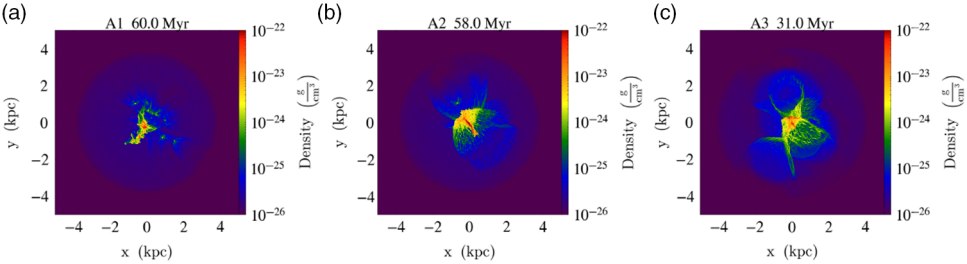


Figure 2. Density-weighted projection plots of gas density distribution at the last snapshots of the three simulations. Left, middle and right panels show model A1 (Salpeter IMF), model A2 (Flat IMF), model A3 (Hirano IMF), respectively.

core radius. We utilize the nine-species (H , H^+ , He , He^+ , He^{++} , e^- , H_2 , H_2^+ , H^-) non-equilibrium chemistry model in *Enzo* to calculate the cooling rate of the primordial gas. We calculate the metal cooling rate following the method of [Glover & Jappsen \(2007\)](#). For star formation and stellar feedback, we follow the model of [Cen & Ostriker \(1992\)](#). We adopt a minimum stellar mass of $1 M_\odot$ with a star formation efficiency of 0.05.

The initial condition of our isolated galaxy is constructed by a spherical cloud of pristine gas with a uniform density profile. SNRs are implemented into the galaxy based on different Pop III IMFs and are added a drift velocity to the SNRs based on the free fall velocity. In this work, we approximate SNRs into spheres and adopt radial physical profiles. We consider three types of them based on the simulations from [Chen *et al.* \(2014, 2015\)](#); core-collapse supernovae (CCSNe), hypernovae, and pair-instability supernovae (PISNe), respectively. The remnants coming from CCSNe have a radius of 500 pc and lowest metallicity and density, the remnants coming from hypernovae have a radius of 1 kpc and intermediate metallicity and density, and the remnants coming from psne have a radius of 1.5 kpc and highest metallicity and density. We adopt three different Pop III IMFs and construct three models (A1, A2 and A3). In model A1, we adopt a Salpeter IMF [Salpeter \(1955\)](#) for the Pop III stars with a peak at $10 M_\odot$. As a result, most of the Pop III stars dies as CCSN. In model A2, we adopt a Flat IMF and thus, the number of different types of SNRs are equal. In model A3, we reference from the cosmological simulation by [Hirano *et al.* \(2015\)](#) that most of the Pop III stars are massive and die as PISN. The initial gas density distribution of the three models is shown in Fig. 1.

3. Results

We show the gas distribution in Fig. 2, the zoomed-in gas density distribution at star-forming sites in Fig. 3, and the stellar mass distribution in Fig. 4 at the last snapshot of the three simulations, respectively. We find that the merging process is different among

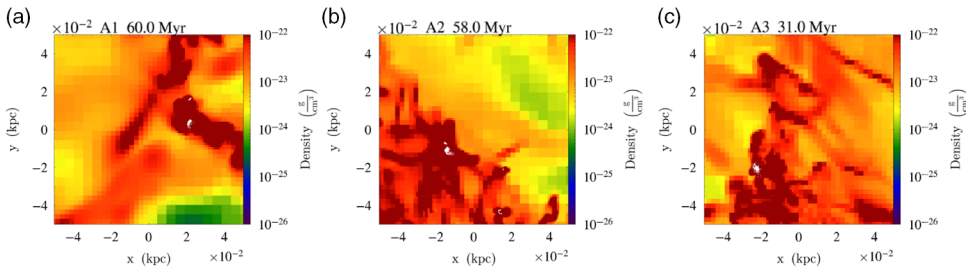


Figure 3. Zoomed-in density-weighted projection plots of gas density distribution at the last snapshots of the three simulations. Left, middle and right panels show model A1 (Salpeter IMF), model A2 (Flat IMF), model A3 (Hirano IMF), respectively. The coordinate of the center of the plot in the left panel is chosen to be (4.6, 4.2, 4.4) kpc from the lower-left corner instead of (5, 5, 5) kpc as in the other two panels.

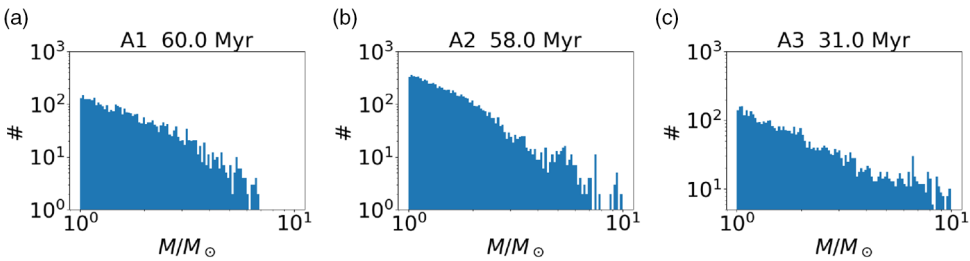


Figure 4. Stellar mass distribution at the last snapshots of three models. Left, middle and right panels show the stellar mass distribution of model A1 (Salpeter IMF), model A2 (Flat IMF), model A3 (Hirano IMF), respectively.

the three models. In model A1, we observe a bar structure appearing in a region deviated from the center. We believe this is because of the asymmetric distribution of the SNRs. When the SNRs merge and collide with each other, part of the gas is squeezed out of the central region of the halo. Therefore, the densest regions and star-forming sites are not in the central part of the halo. In Fig. 3(a), we show the star-forming regions and the white dots represent individual stars. Note that the center of the plot is shifted that it is not the center of the halo anymore. There are $\sim 3,600$ stars at 60 Myr and the resulting stellar mass distribution in this model can be described by a power law. In model A2, the region with highest density remains in the center but we also observe a bar structure along with filaments. In Fig. 3(b), we find more star-forming sites than in model A1. There are over 8,000 stars at 58 Myr. The stellar mass distribution of this simulated galaxy can also be described by a power law with a steeper slope than A1. We find a second peak in the stellar mass distribution that we think it comes from the contribution of star formation in another star-forming site. In this model, we find more star-forming sites. In model A3, the galaxy is initially occupied by the remnants and the region with highest density locates in the center. We observe some filamentary structures in the outer regions where the SNRs collide with each other before entering the central part of the halo. The galaxy has evolved shorter than the other two galaxies but has a much earlier star-forming time. There are $\sim 4,800$ stars at 31 Myr. The stellar mass distribution of this simulation can be described by a power law with a much flatter slope than A1 and A2.

4. Discussion

We perform a series of simulations with various initial conditions based on different assumptions of Pop III IMFs. We find that the star formation history is sensitive to the

initial Pop III IMFs. The slope of the stellar mass distribution is flat when all of the first stars are massive and die as PISN. The Pop II stars in all three models inherit the metallicity information from the first supernovae and their star formation is concentrated in certain regions, because the thermal feedback of Pop II stars is not strong enough to halt the rapid star formation. To resolve the issue, we are implementing a more realistic feedback with radiative transfer to our simulations.

Besides the uniform density profile, we plan to consider the pristine clouds with a gradient density profile to examine the possibility of Pop III star formation in the first galaxies. We will follow the method in Wise *et al.* (2012) to consider Pop III SF and PopII SF separately by adopting the metallicity criterion. If the gas metallicity is $> 10^{-6} Z_{\odot}$, PopII SF is used, and if the metallicity is $< 10^{-6} Z_{\odot}$, Pop III SF is used. We will also investigate the dark matter halos of first galaxies by considering different halo mass and core radius. Our ultimate goal is to develop observational diagnostics for JWST and provide useful insight into the IMF of the first stars.

AKIO INOUE: Do you have any idea to distinguish the three scenarios observationally in the future?

LI-HSIN CHEN: We will be calculating the luminosity of the stars we formed. If we find it being different because the stellar mass distributions differ, we may be able to tell the scenarios apart.

ANDREA MERLONI: How much do you think the dynamical and kinematical initial conditions of your simulation influence the statistical properties of subsequent stellar generations?

LI-HSIN CHEN: I think the dynamics and kinematics have more impact on the star formation site distribution. Unless the dynamics of the turbulence is so strong to change the mixing of the metals. I believe the stellar mass is more related to the cooling, which is affected by the metal content.

Acknowledgements

LHC and KC are supported by the Ministry of Education, Taiwan, R.O.C. under Grant no. MOST 107-2922-I-002-432. and MOST 107-2112-M-001 -044 -MY3. All simulations and analysis were performed on the supercomputer Edison of the National Energy Research Scientific Computing Center (NERSC), a U.S. Department of Energy Office of Science User Facility operated under Contract No. DE-AC02-05CH11231 and the TIARA Cluster at the Academia Sinica Institute of Astronomy and Astrophysics (ASIAA). Computations described in this work were performed using the publicly-available *Enzo* code (<http://enzo-project.org>), which is the product of a collaborative effort of many independent scientists from numerous institutions around the world. Their commitment to open science has helped make this work possible. The analysis and plots were done with yt (Turk *et al.* 2011).

References

- Cen, R. & Ostriker, J. P. 1992, *ApJ*, 399(2), 113
 Chen, K.-J., Heger, A., Woosley, S., Almgren, A., & Whalen, D. J. 2014, *ApJ*, 792, 44
 Chen, K.-J., Bromm, V., Heger, A., Jeon, M., & Woosley, S. 2015, *ApJ*, 802, 13
 Hirano, S., Hosokawa, T., Yoshida, N., Omukai, K., & Yorke, H. W. 2015, *MNRAS*, 448(1), 568
 Glover, S. C. O. & Jappsen, A.-K. 2007, *ApJ*, 666(1), 1
 Salpeter, E. E. 1955, *ApJS*, 121, 1
 Turk, Matthew J., Smith, Britton D., Oishi, Jeffrey S., Skory, Stephen, Skillman, Samuel W., Abel, Tom & Norman, Michael L., *et al.* 2011, *ApJ*, 192, 9
 Wise, J. H., Turk, M. J., Norman, M. L., & Abel, T. 2012, *ApJ*, 745(1), 50